

## SOME ELASTIC MODULI OF THREE THICK COMPOSITES

Emmanuel P. Papadakis, Thadd Patton, Yu-Min Tsai,  
R. Bruce Thompson and Donald O. Thompson

Center for Nondestructive Evaluation  
1915 Scholl Road, Bldg. 2  
Iowa State University  
Ames, Iowa 50011

### INTRODUCTION

Thick composites are in use in critical applications and are proposed for still others. It is important to measure the elastic moduli of thick composites for two reasons: (1) design data on stiffness, and (2) prediction of feasible wave paths for ultrasonic waves for NDE. Except for one earlier report,<sup>(1)</sup> only relatively thin composites of relatively simple symmetries have been measured for their elastic moduli<sup>(2-6)</sup>. Now, it is becoming necessary to measure thick composites of feasible engineering lay-ups. These often provide the complexity of orthorhombic symmetry locally in a specimen combined with curvature in the gross structure. In this work, specimens cut from thick structures will be treated in the same way as crystals to measure the elastic moduli by means of ultrasonic wave velocities. Results on three structures will be presented.

### THEORY

Theory of wave propagation for ultrasonic phase velocity was given in Ref. 1. There, equations were presented to calculate the elastic moduli of an orthorhombic material from the velocities of longitudinal and transverse bulk waves in cut specimens. Illustrations defining the reference axes for the definition of the orthorhombic point group symmetry in relation to the cylinder axes of the macroscopic parts to be tested were also given.

As the parts to be tested are large cylinders before being cut into blocks of various sizes for testing, it is necessary to invoke the theory by Budreck<sup>(7)</sup> to make measurements with the propagation vector in the hoop direction and at angles between the hoop direction and the radial direction. Budreck calculates that the propagation vector remains at a constant angle to the point group symmetry axes as the point group is "wrapped around" the macroscopic symmetry as a cylinder. This theory is illustrated in Fig. 1. Measurements of  $c_{22}$  and  $c_{23}$  would be made utilizing Fig. 1.

In Ref. 1 a difficulty was reported in measuring  $c_{13}$  and  $c_{23}$  in material from an experimental NASA rocket case. Complex values resulted from the very high anisotropy in which the 3-direction (radial) differs greatly from the 1-direction (axial) and the 2-direction (hoop). This difficulty was overcome in some cases in this paper by applying the theory of slowness surfaces to find the Poynting vector direction

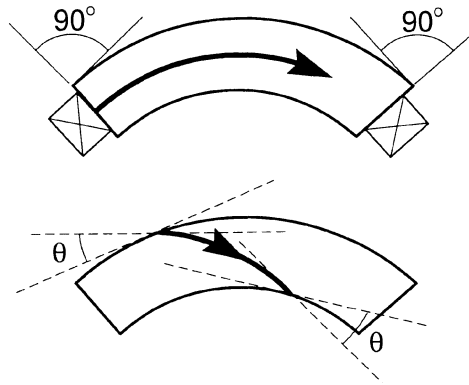


Fig. 1. Pulse propagation directions in curved thick composites.

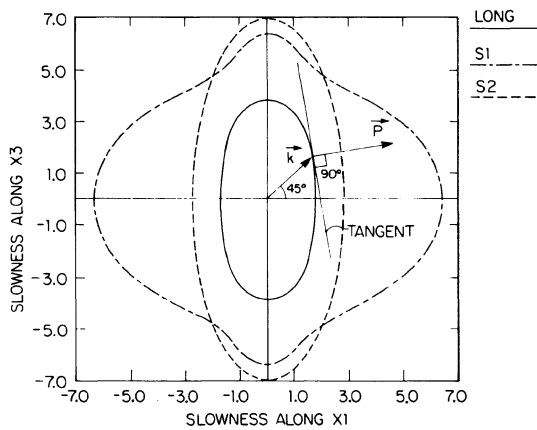


Fig. 2. Slowness surfaces in the 1-3 plane showing the longitudinal Poynting vector  $\mathbf{P}$  for propagation vector  $\mathbf{k}$  at  $45^\circ$  in NASA sample.

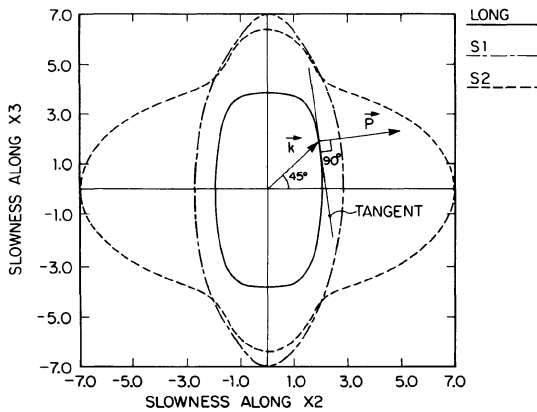


Fig. 3. Slowness surfaces in the 2-3 plane showing the longitudinal Poynting vector  $\mathbf{P}$  for propagation vector  $\mathbf{k}$  at  $45^\circ$  in NASA sample.

corresponding to the input propagation vector direction (defined by the normal to the surface upon which the transmitting transducer was mounted). Calculations<sup>(9)</sup> are shown in Figs. 2 and 3 for the 1-3 plane and the 2-3 plane in the material reported previously.<sup>(1)</sup> Applying the theory,<sup>(9)</sup> one approximates the slowness surfaces by using the previously found values of the diagonal elastic moduli  $c_{jj}$  along with reasonable estimates of the off-diagonal moduli  $c_{ij}$ . The Poynting vector  $\mathbf{P}$  is then along the normal to the tangent to the slowness surface at the point where the propagation vector  $\mathbf{k}$  intersects the slowness surface.<sup>(8)</sup> The theory states that the output transducer should then be on the second sample surface where the Poynting vector  $\mathbf{P}$  would arrive. Then the time is measured, yielding phase velocity when the distance between surfaces is taken along the propagation vector  $\mathbf{k}$ .

## EXPERIMENTAL

### Approach

The approach is to use ultrasonic wave velocities in different directions, combined with density, to measure the elastic moduli. The approach assumes that the composite can be treated analogously to a single crystal of the same point-group symmetry. This symmetry will be determined by the winding angles of the fibers. As the parts of interest are to be cylinders, the approach also assumes that the radius of curvature of the cylinders is much larger than the wall thickness of the cylinders. This is necessary for the definition of the axes with respect to which the elastic moduli are defined. The axes must experience only infinitesimal curvature within a body of dimensions of the order of magnitude of the thickness of the cylinder wall. An analogous approach was used in pyrolytic graphite, an oriented, grown polycrystalline structure.<sup>(10)</sup>

### Specimens

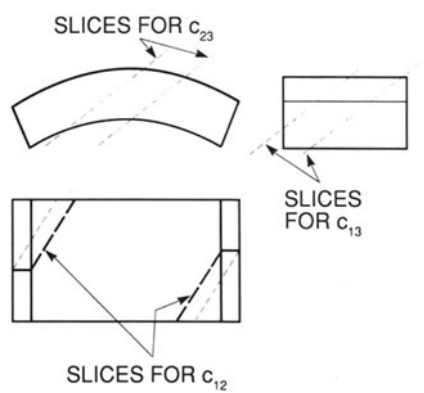
Slabs of a thick (1.25 inch) filament-wound composite from NASA experimental rocket case sections 96 inches in diameter were procured from Hercules<sup>(11)</sup>. Other specimens consisting of segments cut from cylinders made for the Navy were also procured.<sup>(12)</sup> The full-size cylinders had been 8 inches long, 8 inches diameter, and 5/8 inch thick. The lay-ups of the Navy composites were

Sample #1	[ 90 4 0 2 ] <sub>13</sub> 90 <sub>3</sub>
Sample #2	[ 90 2/0 2/+45 2/-45 ] <sub>10</sub> 90

while the lay-up of the NASA rocket case composite was much more complex and is given in Table 1. Details of the shape of the cut samples from the latter material were given in Ref. 1. A drawing of the sample configuration for the Navy material is shown in Fig. 4. In some cases the angle  $\theta$  for propagation direction  $\mathbf{k}$  on a diagonal between axes of a specimen was not  $45^\circ$  as it had been in Ref. 1. For non- $45^\circ$  directions, Equations 9, 12, and 15 in Ref. 1 should be modified to read " $1/\sin\theta \cos\theta$ " instead of " $2$ " in front of the radical sign, since insertion of  $45^\circ$  for  $\theta$  led to the value 2.0 for the true expression  $1/\sin\theta \cos\theta$ .

### Ultrasonic System

The ultrasonic system is shown in Fig. 5. Through-transmission measurements were employed, as the attenuation was too high to make pulse-echo measurements. Broadband transducers of frequencies 1 MHz at 1/2-inch diameter and 1/2 MHz at 1-inch diameter were used. The pulser-receiver provided the trigger pulse to the CRO and the high-voltage pulse to the transmitting transducer; then received and amplified the transmitted ultrasonic signal for the Y-axis display. The measuring oscilloscope provided two indicators between which the delay time was measured. The indicators were set on the leading edge of the output pulse and on the peak of the first half cycle of the received signal. A differential measurement was made by first measuring the specimen and the glass buffer combined in series and then measuring only



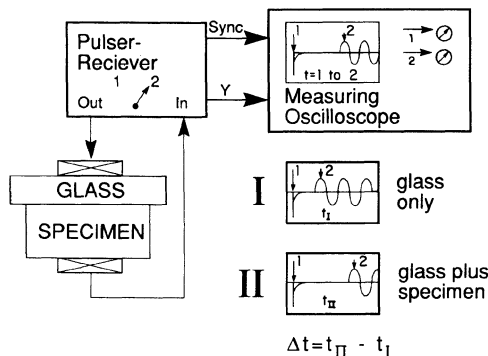


Fig. 5. Ultrasonic system for measurements. Panametrics 5052 PR pulser-receiver and LeCroy 9400 digital oscilloscope.

the glass buffer. This differential measurement accounted for two systematic errors<sup>(10)</sup>: (1) utilization of the leading edge of the input pulse, and (2) delay in the transducer wear plates.

### Measurements

The ultrasonic delay within the specimens was measured for each wave listed in Table 1 of Ref. 1 according to the method given above with two exceptions. (a) For the more highly curved blocks 5/8 inch thick, longitudinal waves in the "3" direction were measured by pulse-echo in a water bath, (b) For blocks cut for propagation at an angle  $\theta$  with respect to "3" axis to obtain  $c_{13}$  and  $c_{23}$ , the technique described in the Theory section for locating the Poynting vector was implemented as follows:

It was desired to place the receiving transducer at the location corresponding to the arrival of the Poynting vector as shown in Fig. 6.

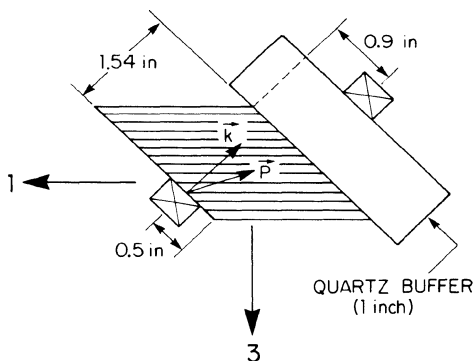


Fig. 6. Diagram showing the positioning of the receiving transducer to account for the arrival of the Poynting vector as it deviates from the propagation vector.

Table 2. Results of Velocity Measurements  
( $f = 1.0$  MHz, Velocities in cm/ $\mu$ s, moduli in  $10^{11}$  dyn/cm<sup>2</sup>)

Velocity Name, Ref. 1	Elastic Modulus	NASA		Navy #1		Navy #2	
		Velocity	Modulus	Velocity	Modulus	Velocity	Modulus
$v_{L1}$	$c_{11}$	0.580	4.73	0.664	7.19	0.650	6.43
$v_{L2}$	$c_{22}$	0.510	3.66	0.883	12.72	0.681	7.06
$v_{L3}$	$c_{33}$	0.260	0.954	0.294	1.41	0.306	1.42
$v_{T21}$		0.367	avg.	0.221	avg.	0.396	avg.
$v_{T12}$	$c_{66}$	0.352	1.82	0.225	0.811	0.346	2.09
$v_{T13}$		0.150	avg.	0.167	avg.	0.177	avg.
$v_{T31}$	$c_{55}$	0.163	0.344	0.159	0.436	0.185	0.498
$v_{T23}$		0.134	avg.	0.170	avg.	0.175	avg.
$v_{T32}$	$c_{44}$	0.153	0.290	0.196	0.546	0.179	0.456
$v_{L1-2}$		0.616	2.81	0.658	1.15	0.667	2.49
		0.438	0.786	N/A	N/A	N/A	N/A
		0.382	0.375	N/A	N/A	N/A	N/A
Density		1.407		1.631		1.522	

The deviation of the Poynting vector is toward the ply direction since the velocity is faster along the plies than normal to them. This effect was observed experimentally by noting that the received intensity (observed voltage output of the transducer) was highest at a location corresponding to the point of arrival of the Poynting vector. The direction found by intensity agreed with the direction calculated by theory. Delay was then measured.

Density was measured by measuring the dimensions and the mass of rectangular pieces.

The phase velocities were calculated as distance divided by time where the distance was the thickness of a specimen along the propagation vector  $k$  and the time was the measured delay in the specimen. The moduli were calculated from the velocities and the density by the formulas in Eqs. (3) - (17) in Ref. 1 as cross-referenced in Table 1 of Ref. 1. The velocities, moduli, and density are reported in Table 2.

It was not possible to measure the time delays in the small specimens of the Navy material cut at angles for propagation between the 1 & 3 axes and between the 2 & 3 axes. Further work will be required on methodologies to find  $c_{13}$  and  $c_{23}$ .

The elastic moduli for the NASA material given in Table 2 are shown in matrix form here in units of  $10^{11}$  dynes/cm<sup>2</sup>.

4.73	2.81	0.786	0	0	0
2.81	3.66	0.375	0	0	0
0.786	0.375	0.954	0	0	0
0	0	0	0.290	0	0
0	0	0	0	0.344	0
0	0	0	0	0	1.82

The large anisotropy of the thick composite material is evident as is its orthorhombic point-group symmetry. For units of GPa, multiply each number by 10.

The moduli  $c_{13}$  and  $c_{23}$ , where found, were entered into the slowness surface calculations to obtain the final slowness surfaces shown in Figs. 2 and 3.

It should be noted that the lack of windings in the  $\pm 45^\circ$  or in the  $\pm 33^\circ$  directions in Navy Specimen #1 (Only  $0^\circ$  and  $90^\circ$  windings) results in low values of  $c_{12}$  and  $c_{66}$ . This is consistent with a model  $90^\circ$  X-shaped overlaps of fibers instead of triangularly stiffened overlaps in the other specimens.

The results given above are not all of equal accuracy. First, the shear wave measurements of delay were perturbed somewhat (but less than  $\tau/4$  of the 0.5 MHz wave) by the presence of a leading longitudinal wave generated as an edge effect in the shear-poled potted piezoelectric ceramic transducers. Hence,  $c_{44}$ ,  $c_{55}$ , and  $c_{66}$  are not as accurate as  $c_{11}$ ,  $c_{22}$ , and  $c_{33}$  which have maximum errors of the order of  $\pm 2\%$  due to the measurements. Probably the shear moduli on the matrix diagonal are good to  $\pm 8\%$  or  $\pm 12\%$  at worst. This estimate is derived from Table 3 where certain velocities which should be equal are not equal in practice, such as  $v_{T21}$  and  $v_{T12}$ . Beyond that, the off-diagonal terms are less accurate because of the small differences between relatively large terms encountered in the calculations in Eqs. (9), (12), and (15). Errors of  $\pm 25\%$  would not be surprising.

#### ACKNOWLEDGEMENTS

This work was supported by the U.S. Navy through the University of Illinois (Contract #N0014-86-K-0799) and was performed by the Center for NDE at the Ames Laboratory. Ames Laboratory is operated for the U.S. Department of Energy by Iowa State University under Contract No. W-7405-ENG-82. The findings, opinions, and recommendations expressed in this paper are those of the author and not necessarily those of the University of Illinois or the U.S. Navy.

#### REFERENCES

1. E. P. Papadakis, T. Patton, Y.- M. Tsai, and D. O. Thompson, "The Elastic Moduli of Thick Composites," in Rev. Prog. QNDE, Vol. 9B, ed. by, D. O. Thompson and D. E. Chimenti, Plenum, New York, 1990, pp. 1387-1394.
2. R. D. Kritz and W. W. Stinchcomb, "Elastic Moduli of Transversely Isotropic Graphite Fibers and Their Composites", Experimental Mechanics **19**, 41-49 (Feb. 1979).
3. J. E. Zimmer and J. R. Cost, "Determination of the Elastic Constants of a Unidirectional Fiber Composite Using Ultrasonic Velocity Measurements", J. Acoust. Soc. Amer. **47**, 795-803 (1970).
4. W. H. Prosser, "Ultrasonic Characterization of the Nonlinear Elastic Properties of Unidirectional Graphite/Epoxy Composites", NASA Contractor Report #4100, (Oct. 1987), pp. 48-65.

5. R. E. Smith, "Ultrasonic Elastic Constants of Carbon Fibers and Their Composites", J. Appl. Phys. 43 (6), 2555-2561 (June 1972).
6. T. R. Taichert and A. N. Guzelsu, "Measurements of Elastic Moduli of Laminated Composites Using an Ultrasonic Technique", J. Composite Materials 5, 549-552 (Oct. 1971).
7. D. E. Budreck, "Pulse Propagation in Cylindrically Wound Thick Composite Specimens," in Rev. Prog. QNDE, Vol. 9A, ed. by D. O. Thompson and D. E. Chimenti, Plenum, New York, 1990, pp. 181-188.
8. B. A. Auld, Acoustic Fields and Waves in Solids, Vol. I, John Wiley & Sons, New York, 1973, pp. 221-225.
9. A Minachi, Center for NDE, Iowa State University, private communication.
10. E. P. Papadakis and H. Bernstein, "Elastic Moduli of Pyrolytic Graphite," J. Acoust. Soc. Amer. 35, 521-524 (1963).
11. W. Murri, Hercules Aerospace Co., private communication.
12. H. Garala, David Taylor Research Center, private communication.